nature biotechnology

Translation efficiency of mRNAs is increased by antisense oligonucleotides targeting upstream open reading frames

Xue-hai Liang[1], Wen Shen[1], Hong Sun[1], Michael T Migawa[2], Timothy A Vickers[1] & Stanley T Crooke[1]

Increasing the levels of therapeutic proteins *in vivo* remains challenging. Antisense oligonucleotides (ASOs) are often used to downregulate gene expression[1] or to modify RNA splicing[2,3], but antisense technology has not previously been used to directly increase the production of selected proteins. Here we used a class of modified ASOs that bind to mRNA sequences in upstream open reading frames (uORFs) to specifically increase the amounts of protein translated from a downstream primary ORF (pORF). Using ASO treatment, we increased the amount of proteins expressed from four genes by 30–150% in a dose-dependent manner in both human and mouse cells. Notably, systemic treatment of mice with ASO resulted in an ~80% protein increase of LRPPRC. The ASO-mediated increase in protein expression was sequence-specific, occurred at the level of translation and was dependent on helicase activity. We also found that the type of RNA modification and the position of modified nucleotides in ASOs affected translation of a pORF. ASOs are a useful class of therapeutic agents with broad utility.

Selective increase of the levels of specific proteins has been a therapeutic goal for almost 40 years. Substantial effort has been made using approaches such as gene therapy and antisense-mediated de-repression by targeting inhibitory antisense transcripts, with only partial success, owing to obstacles in safe delivery, immune responses or the limited number of applicable genes[4–7]. Approaches that are useful for a broad range of genes are needed to safely and specifically increase the levels of endogenous proteins. One potential approach is to increase the translational efficiency of specific mRNAs.

In eukaryotic cells, translation is usually initiated via a cap-dependent process. The preinitiation complex binds at the 5′ cap of an mRNA and scans the 5′ untranslated region (UTR) for the presence of an AUG start codon[8–10]. Many factors in 5′ UTRs, such as structures, protein-binding sites, kozak sequence and internal ribosome entry site, can regulate translation[10–14]. Recently, uORFs have also been shown to regulate translation efficiency of pORFs[15,16]. Approximately 50% of human mRNAs have AUGs upstream of the primary AUG (pAUG)[17,18], the start codon for the main protein product of the mRNA. In many cases, translation of uORFs inhibits translation from the pAUG, likely by reducing its accessibility to the preinitiation complex. Mutations in 5′ UTRs can create or disrupt uORFs, thus affecting pORF translation[17]. Many characteristics, including the numbers and lengths of uORFs, the strength of the Kozak sequence and the position of uORFs in the 5′ UTR, affect the regulatory impact of uORFs[15,16].

Because protein production can be reduced by translation of uORFs, we reasoned that a properly designed ASO that inhibits uORF translation without causing degradation of the mRNA might increase translation of the pORF. Initially we designed five ASOs with 2′-*O*-methyl (Me) modifications and phosphodiester (PO) linkages. These PO-Me ASOs were complementary to the uAUG region of human *RNASEH1* mRNA, encoding RNase H1 (**Fig. 1a**), which contains a functional uORF[19]. We transfected ASOs into HeLa cells for 24 h, and analyzed RNase H1 protein, which is moderately expressed, by western blot (**Fig. 1b**). Three ASOs increased the protein level by 40–66%, whereas the other two ASOs had no effect. The ASOs did not substantially affect *RNASEH1* mRNA levels (**Supplementary Fig. 1a**), indicating that uORF-targeting ASOs increased pORF protein levels in a position-dependent manner. The increased RNase H1 protein caused by treatment with the uORF ASO was functional, as transfection of cells with ASO-761909 (all ASOs are listed in **Supplementary Note**), but not the control ASO-759704, increased antisense activities of oligonucleotides designed to direct RNase H1 cleavage of two different RNAs (**Supplementary Fig. 1b**,**c**) that have been described previously[20]. In addition, the uORF ASO effect was not unique to HeLa cells, as ASO-761909 also increased RNase H1 protein levels in HEK293 cells (**Supplementary Fig. 1d**).

The uORF ASOs were highly specific as shown by following experiments: (i) whereas uORF ASO-761909 increased protein levels dose-dependently, a control ASO targeting a mouse mRNA had no effect on RNase H1 protein levels (**Fig. 1c**,**d**); (ii) ASOs with 2-nucleotide (nt) mismatches relative to the ASO-761909 at or near the uAUG binding region showed substantially reduced activity (**Fig. 1e**), further supporting a position-dependent mechanism and specificity; (iii) the effect of the ASO-761909 was inhibited by transfection of a complementary oligonucleotide (ASO-761929) (**Fig. 1f**); this treatment did not substantially affect *RNASEH1* mRNA levels (**Supplementary Fig. 2a**); (iv) treatment with ASO-761909 did not affect global translation, as demonstrated by pulse-chase labeling of nascent proteins (**Supplementary Fig. 2b**); and (v), although ER stress can selectively increase translation of some uORF-containing mRNAs[16], treatment with ASO-761909 did not cause ER stress, as shown by unchanged phosphorylated eIF2α protein (**Supplementary Fig. 2c**).

[1]Department of Core Antisense Research, Ionis Pharmaceuticals, Inc., Carlsbad, California, USA. [2]Department of Medicinal Chemistry, Ionis Pharmaceuticals, Inc., Carlsbad, California, USA. Correspondence should be addressed to X.L. (lliang@ionisph.com).

Received 4 June 2015; accepted 2 May 2016; published online 11 July 2016; doi:10.1038/nbt.3589

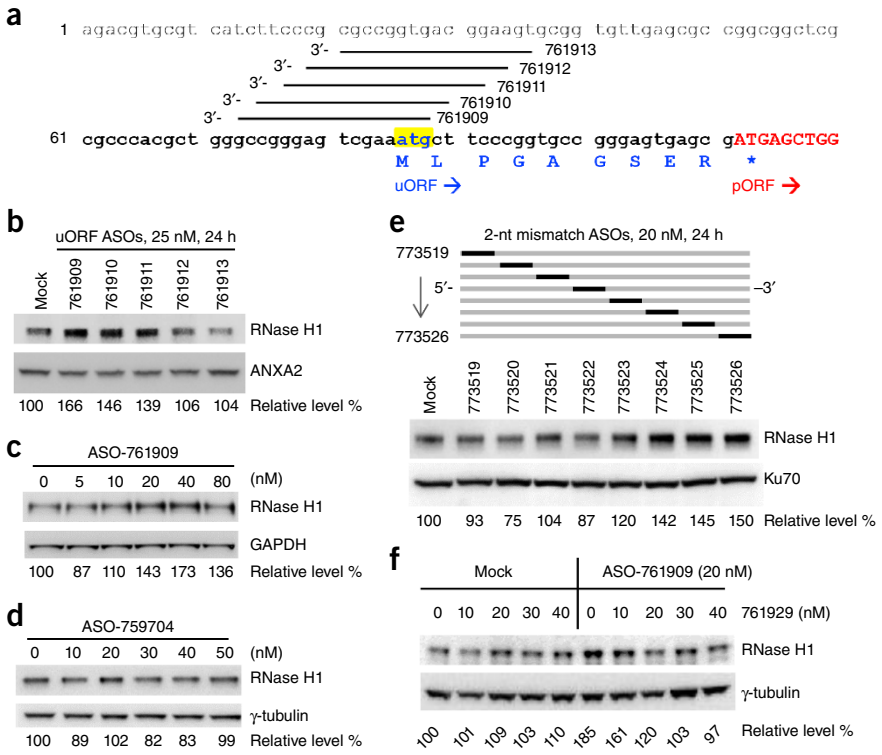

Figure 1 Antisense ASOs targeting the uAUG region specifically increased protein production from the pORF. (**a**) Sequence of *RNASEH1* 5′ UTR and positions of uORF ASOs. (**b**) Western blot of RNase H1 in HeLa cells treated with different ASOs for 24 h. (**c**) Western blot of RNase H1 in HeLa cells treated for 24 h with indicated concentrations of ASO-761909. (**d**) Western blot of RNase H1 in HeLa cells treated for 24 h with a control ASO-759704. (**e**) Western blot of RNase H1 in HeLa cells treated for 24 h with ASOs carrying 2-nt mismatches at positions indicated by black lines above the blot. (**f**) Western blot of RNase H1 in HeLa cells that were mock-transfected or transfected with 20 nM ASO-761909 for 5 h, and transfected again with indicated concentrations of a complementary oligonucleotide 761929 for an additional 5 h. Tubulin, GAPDH, Ku70 or ANXA2 proteins were detected as loading controls as indicated. Numbers below blots indicate normalized ratios of RNase H1 protein compared to control sample. All experiments were repeated at least two times and representative results are shown. Full-length blots are presented in **Supplementary Figure 10**.

It is known that antisense technologies commonly used to degrade complementary RNAs can cause off-target reduction of RNAs base-pairing with the antisense molecules[21], but uORF ASOs should have minor off-target effects because this type of ASO does not support RNA cleavage activities. Indeed, although ASO-761909 can potentially interact with eight off-target RNAs via imperfect base pairing (>11 bp), the levels of these mRNAs were not substantially affected by ASO treatment (**Supplementary Fig. 2d**,**e**). Notably, the protein levels of two tested off-target genes (*SPPL2B* and *FGFR1*) also were not affected (**Supplementary Fig. 2f**). We confirmed minimal off-target effects at a global level by microarray analyses (Gene Expression Omnibus accession number GSE76343). Under the experimental conditions where RNase H1 protein level was increased by treatment with uORF ASO-761909 (15 h after transfection at 30 nM concentration), only 22 genes and 13 genes exhibited significantly increased or reduced expression (absolute $\log_2$ ratio>1, $P < 0.05$), respectively, as compared with mock transfected cells (**Supplementary Table 1**). Similar treatment with a control ASO-761932 (30 nM, 15 h) also showed very minor off-target effect, with 42 genes and 39 genes significantly upregulated or downregulated (**Supplementary Table 2**). Furthermore, the minimal changes in expression did not correlate with potential complementary sequence to the ASOs. Together, these results suggest that the increase of RNase H1 protein level was unlikely caused by indirect effects of altered expression of other genes.

The affinity of ASOs for target RNA sequence (measured by melting temperature, T_m) is affected by properties intrinsic to the ASO, including the number of base pairs, the numbers and positions of mismatches, and chemical modifications. Numerous modifications have been created to enhance the drug properties of ASOs. The phosphorothioate (PS) backbone modification reduces T_m by ~0.5 °C per modification but imparts nuclease resistance. The 2′-*O*-methyl, 2′-*O*-methoxyethyl (MOE) and constrained-ethyl (cEt) modifications increase T_m[22,23].

We analyzed the effects of length and chemical composition on the activity of uORF ASOs targeting *RNASEH1*. Both a 16-mer PS-MOE ASO-759304 (T_m = 82.5 °C) and an 18-mer PS-Me ASO-783679 (T_m = 82.1 °C) dose-dependently increased RNase H1 protein levels (**Fig. 2a**,**b**) without affecting *RNASEH1* mRNA levels (data not shown). Protein levels increased 8 h after ASO-759304 transfection and stopped increase 60 h after transfection (**Supplementary Fig. 3a**), likely owing to low levels of translation in the confluent cells[24]. The optimal lengths for ASOs modified at each nucleotide with PS-MOE, PS-Me or PO-Me ASOs were 18 nt (T_m > 90 °C), 12–16 nt (T_m = 60–82 °C) and 16 nt (T_m = 81 °C), respectively (**Fig. 2c–f**). However, treatment of cells with 16-mer (T_m > 90 °C) or 20-mer (T_m > 90 °C) uniformly PO-MOE-modified ASOs reduced RNase H1 protein levels and elevated *RNASEH1* mRNA levels (**Supplementary Fig. 3b–d**). These results suggest that the ASO affinity has an important role, but the nature of modification is also influential. Indeed, when we enhanced the affinity even further by adding three cEts to the 5′ end, but not the 3′ end, of the 16-mer PO-MOE ASO, the activity reduced (**Fig. 2g**). We observed enhanced ASO activity when we increased the number of cEts from two to four at the 3′ end of a 16-mer PS-Me ASO (**Fig. 2h**). Thus, ASO affinity is important in the observed enhancement of translation, but the types and positions of chemical modifications are also influential.

ASO-761909 treatment did not alter the level or splicing pattern of *RNASEH1* pre-mRNA (**Supplementary Fig. 4a**,**b**). In addition, the cytoplasmic-nuclear distribution and the length of poly(A) tail of mature *RNASEH1* mRNA were not affected (**Supplementary Fig. 4c**,**d**). Finally, RNase H1 protein stability appeared normal in ASO-treated cells, as determined by cycloheximide treatment (**Fig. 3a**,**b**). These results strongly suggest that the uORF ASO increased RNase H1 protein at the translational level. Indeed, ASO-761909 treatment specifically shifted *RNASEH1* mRNA, but not control *PTEN* mRNA, toward polysomes, as shown by mRNA polysome profile (**Supplementary Fig. 5**) and the increased ratio of *RNASEH1* mRNA in polysome vs. mono-ribosome fractions (**Fig. 3c**). In addition, inhibition of cap-dependent translation by treatment with a small molecule 4E1Rcat

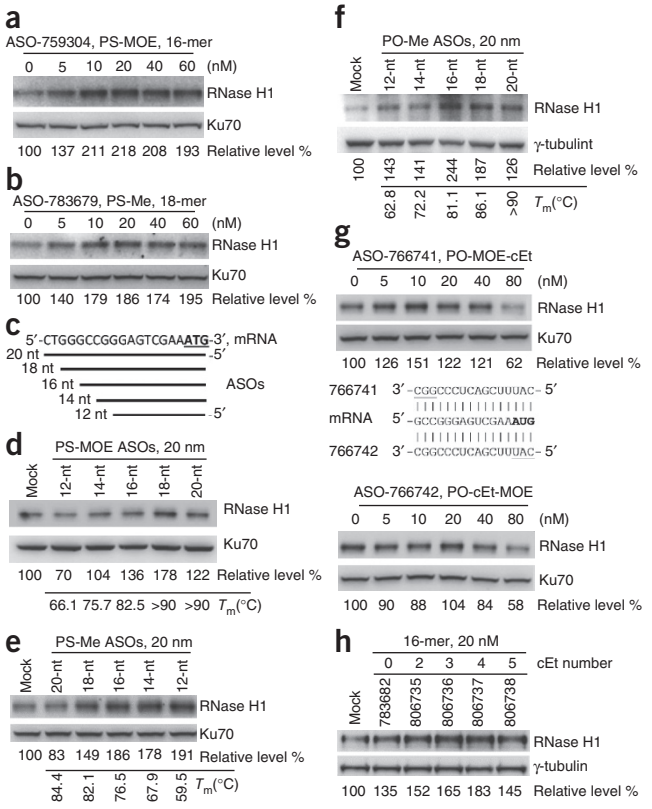

Figure 2 ASO modification and length effects on RNase H1 protein level. (**a**,**b**) Western blot of RNase H1 in HEK293 cells transfected with ASOs with PS-MOE (**a**) or PS-Me (**b**) modifications for 10 h. (**c**) Schematics of ASOs of different lengths. (**d**–**f**) Western blot of RNase H1 in HEK293 cells treated for 10 h with ASOs of different lengths containing PS-MOE (**d**), PS-Me (**e**). or PO-Me (**f**). Measured ASO T_m is listed below the blots. (**g**) Western blot of RNase H1 protein levels in HEK293 cells treated for 10 h with ASOs containing mixed modifications. (**h**) Western blot of RNase H1 in HEL293 transfected for 10 h with PS-Me ASOs with different numbers of cEt substitutes at 3′ end. Numbers below blots are estimated ratios of RNase H1 protein levels compared to control sample. Ku70 or tubulin served as loading controls. All experiments were repeated two or more times, and representative results are shown. Full-length blots are presented in **Supplementary Figure 11**.

that inhibits interaction between eIF4E and eIF4G abolished uORF ASO activity (**Fig. 3d**), suggesting that uORF ASOs result in cap-dependent translation. Several attempts to immunoprecipitate nascent RNase H1 protein were unsuccessful, most likely owing to low abundance and lack of a highly specific antibody. However, we detected uORF-ASO-induced translational increase of proteins for another tested protein, LRPPRC (see below).

Because we designed the uORF ASOs to base pair with 5′ UTRs of targeted mRNAs[25], and RNA helicases, such as DHX29, are involved in resolving the 5′ UTR structures during scanning process[26], we evaluated the effect of DHX29 on uORF ASO activity. DHX29 protein level was reduced using two siRNAs with different activities (**Fig. 3e**). Under the experimental conditions, DHX29 protein reduction itself did not substantially affect the level of RNase H1 protein (**Fig. 3f**). However, we observed decreased activity of uORF ASO-761909 upon DHX29 protein reduction, and the ASO even reduced RNase H1 protein level in cells with greater reduction of DHX29 protein by siRNA si-03 (**Fig. 3f**). These results suggest that the uORF-ASO-induced protein production requires DHX29 for removal of the ASOs from mRNA, although it is possible, but less likely, that DHX29 may facilitate ASO binding to mRNA. With deficient helicase or with high ASO affinity (such as PO-MOE ASO-783675), the uORF ASOs may inhibit scanning by the preinitiation complex.

This hypothesis is supported by structural probing of *RNASEH1* mRNA using dimethyl sulfate (DMS). There were no differences in DMS reactivity patterns of the uORF region in cells transfected with the uORF ASO-761909 and in mock-transfected cells (**Fig. 3g**), suggesting that the ASO was removed from the RNA in these cells. We detected differences in cells transfected with ASO-783675, the high affinity PO-MOE ASO that caused a reduction in RNase H1 protein levels. These results suggest that active uORF ASOs hinder, but do not completely block, the scanning process; this leads to bypass of the uAUG, enhancing initiation at the pAUG. This model also explains the initial observation that active uORF ASOs have reduced activity or even decreased protein levels at high doses compared to lower doses, leading to bell-shaped dose-response curves in some cases. It is possible that high concentrations of ASOs make it difficult for helicase(s) to remove all ASOs associated with mRNA at a given time, resulting in less pORF translation. This speculation is supported by the fact that in subsequent studies we found that by optimizing the affinity of the ASO it is possible to avoid such bell-shaped curves (**Fig. 2a**,**g**, and data not shown).

Although the exact mechanism is not fully understood, our results suggest that the ASO-mediated increase in protein occurs at the translational level, most likely involving ASO-mRNA base pairing. This view is supported by observations from a dual-luciferase reporter assay for RNase H1 uORF. A uAUG→uUUG mutation led to a ~5.5-fold increase of the luciferase activity, whereas a 7-nt mutation at sequences upstream from uAUG had only a slight effect (**Supplementary Fig. 6a–d**), indicating translation initiation from uAUG, but not protein binding or mRNA structure at this region, has a major role in inhibiting RNase H1 translation. Indeed, treatment with ASO-761909 (one mismatch) or ASO-773517 (match) had no effect on luciferase activity for the uUUG reporter (**Supplementary Fig. 6e**). However, the matched ASO-761909, but not a mismatched ASO-865495, increased translation for the reporter containing wild-type *RNASEH1* sequence (**Fig. 3h**). Consistently, for a reporter containing a 7-nt compensatory mutation at the ASO binding site, the now-matched ASO-865495, but not the now-unmatched ASO-761909, increased luciferase activity (**Fig. 3h**). Furthermore, stepwise increase of mismatches from one to four in the uORF ASO binding region (M1–M4) of the luciferase reporter gradually reduced the activity of ASO-761909 (**Supplementary Fig. 6f**,**g**), whereas increasing base-pairing using a mutant ASO (XL695) progressively restored ASO activity (**Supplementary Fig. 6h**,**i**). We repeated these experiments five times with different doses and observed similar trends (data not shown).

To determine whether uORF ASOs can enhance translation of other genes, we designed ASOs to three additional genes: human *SFXN3*, mouse *Mrpl11*, and mouse *Lrpprc*, which have been previously shown to contain uORFs that reduce translation by 60–80%[17]. These mRNAs have different uORF characteristics, such as the length and position of uORFs, the strength of kozak consensus sequence, or overlap or no overlap with pORFs (**Supplementary Fig. 7a**).

An ASO targeting *SFXN3* uORF dose-dependently increased the level of protein by ~35%, but not of mRNA, in HeLa cells (**Fig. 4a** and **Supplementary Fig. 7b**,**c**). A 2-nt mismatch to the uAUG region substantially reduced ASO activity (**Supplementary Fig. 7d**). In addition, a uORF ASO-773534 targeting *Mrpl11* dose-dependently increased

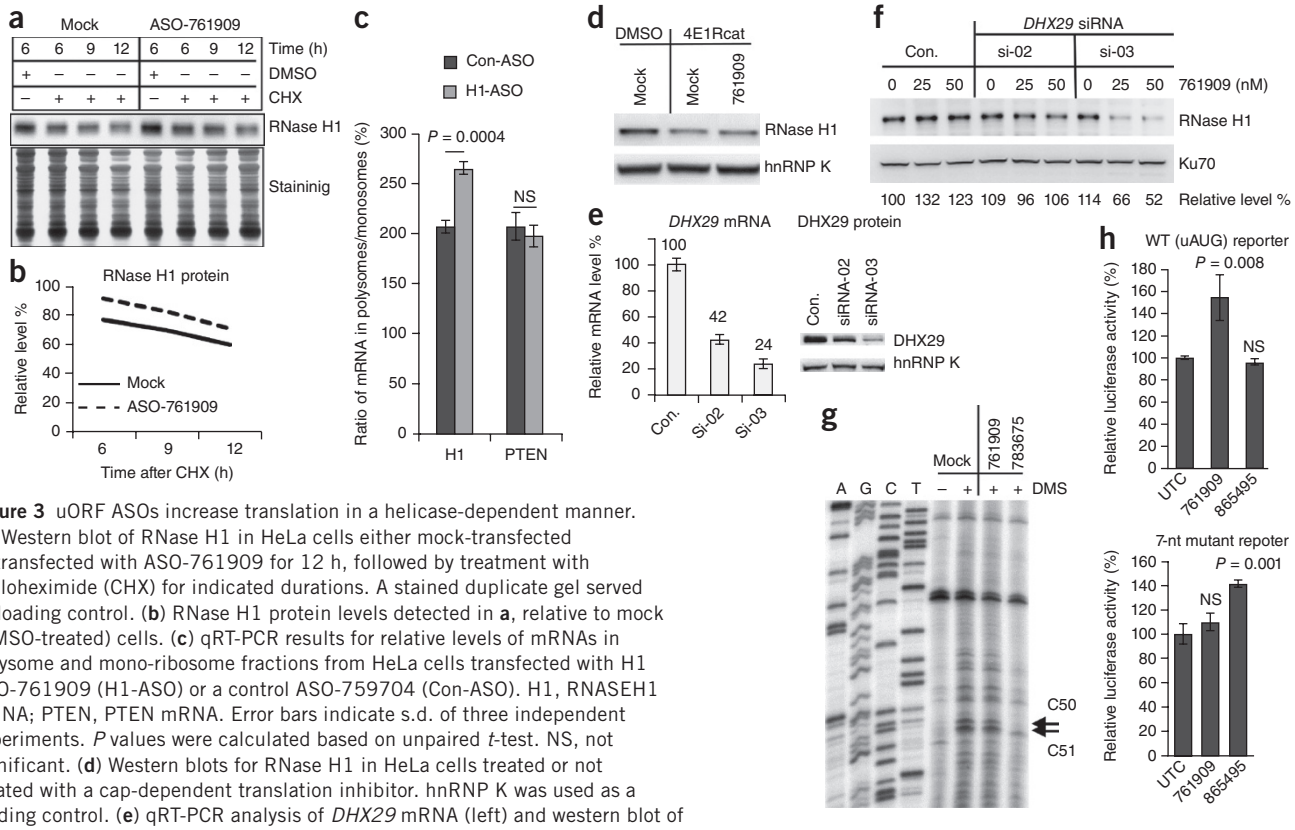

Figure 3 uORF ASOs increase translation in a helicase-dependent manner. (**a**) Western blot of RNase H1 in HeLa cells either mock-transfected or transfected with ASO-761909 for 12 h, followed by treatment with cycloheximide (CHX) for indicated durations. A stained duplicate gel served as loading control. (**b**) RNase H1 protein levels detected in **a**, relative to mock (DMSO-treated) cells. (**c**) qRT-PCR results for relative levels of mRNAs in polysome and mono-ribosome fractions from HeLa cells transfected with H1 ASO-761909 (H1-ASO) or a control ASO-759704 (Con-ASO). H1, RNASEH1 mRNA; PTEN, PTEN mRNA. Error bars indicate s.d. of three independent experiments. *P* values were calculated based on unpaired *t*-test. NS, not significant. (**d**) Western blots for RNase H1 in HeLa cells treated or not treated with a cap-dependent translation inhibitor. hnRNP K was used as a loading control. (**e**) qRT-PCR analysis of *DHX29* mRNA (left) and western blot of DHX29 protein (right) in HeLa cells treated with different small interfering (si)RNAs. Con., cells treated with control siRNA; Si-02 and Si-03, cells treated with DHX29-specific siRNAs Si-02 and Si-03, respectively. hnRNP K served as a control for loading in western blot. (**f**) Western blot for RNase H1 protein in cells treated for 24 h with different siRNAs, followed by transfection of the uORF ASO. Ku70 served as a loading control. Relative RNase H1 protein levels were quantified and listed below the lanes. (**g**) RNA structure probing of RNase H1 5′ UTR region using DMS modification and primer extension. A DNA sequencing reaction was performed using the same primer. The nucleotides with altered structures are indicated. All experiments were repeated at least two times and representative results are shown. (**h**) Luciferase activities in cells transfected with wild-type (WT; top panel) or 7-nt mutant (bottom panel) reporter plasmids followed by treatment with ASOs for 10–16 h. Luciferase experiments were repeated more than five times and representative results are shown. The error bars are s.d. of three independent experiments. *P* values were calculated based on unpaired *t*-test. NS, not significant. Full-length blots are presented in **Supplementary Figure 12**.

protein, but not mRNA, levels in mouse b.End.3 cells (**Fig. 4b** and **Supplementary Fig. 8a**,**b**). We confirmed this effect using a dual-luciferase reporter assay. ASO-773534, but not a control ASO, increased luciferase activity (**Supplementary Fig. 8c**).

We observed increases in protein abundance when we targeted the uORF of *Lrpprc* mRNA (**Supplementary Fig. 9a**) in the mouse MHT cell line[27]. PO-Me uORF ASOs of 16-mer, 18-mer or 20-mer increased the LRPPRC protein level ~2.5-fold compared to mock-transfected cells (**Fig. 4c**,**d** and **Supplementary Fig. 9b**), without substantially affecting *Lrpprc* mRNA levels (**Supplementary Fig. 9c**). To confirm that uORF ASOs increased translation, we performed pulse-chase labeling and immunoprecipitation, and found that nascent LRPPRC protein levels were substantially increased in ASO-761930-treated MHT cells (**Fig. 4e**).

To ascertain whether uORF ASOs can increase translation of proteins in animals, we treated mice with an 18-mer PS-Me ASO (ASO-761933) targeting the *Lrpprc* uORF that increased LRPPRC protein levels in MHT cells (**Fig. 4f**). The ASO-761933 increased amounts of LRPPRC protein by approximately 37% in mouse liver at 48 h after subcutaneous injection (75 mg/kg) compared to protein levels in animals treated with vehicle ($P = 0.0078$, 95% confidence interval (CI): 13.73% to 60.23%), whereas a control ASO-809793 had no obvious effect (**Fig. 4g**,**h** and **Supplementary Fig. 9d**). In addition, we performed the *in vivo* dose-response study twice ($n = 3$ for each dose in each study) and obtained similar protein upregulation results (**Fig. 4i** and **Supplementary Fig. 9e**). In this case, we obtained ~82% ($P = 0.0093$, 95% confidence interval (CI): 35.17% to 129.15%) and ~71% ($P = 0.01$, 95% CI: 32.25% to 109.65%) increase of LRPPRC protein when we dosed ASO-761933 at 25 mg/kg and 50 mg/kg, respectively. Similar to some *in vitro* studies, the ASO effect was reduced at very high concentrations in animals. In structure-activity relationship (SAR) studies, we found that by optimizing the affinity of the ASO it is possible to avoid such effects (**Fig. 2a**,**g** and data not shown).

Our results indicate that ASOs targeting uORFs can sequence-specifically increase protein levels both *in vitro* and *in vivo*. As uORFs are present in a large number of mRNAs[16,28], ASO-based agents can thus be used to specifically increase endogenous protein production for many genes. As many diseases result from decreased protein levels, this approach may find application in biological research and in the clinic, as ASOs have been well-developed for efficient and safe delivery. The level of increase we observed (30–150%) is meaningful, because the degree of increase was based on normal protein levels. In patients with loss of function, the basal levels of target proteins are low, thus higher fold change is expected. On the other hand, even modest increase of functional proteins could be therapeutically

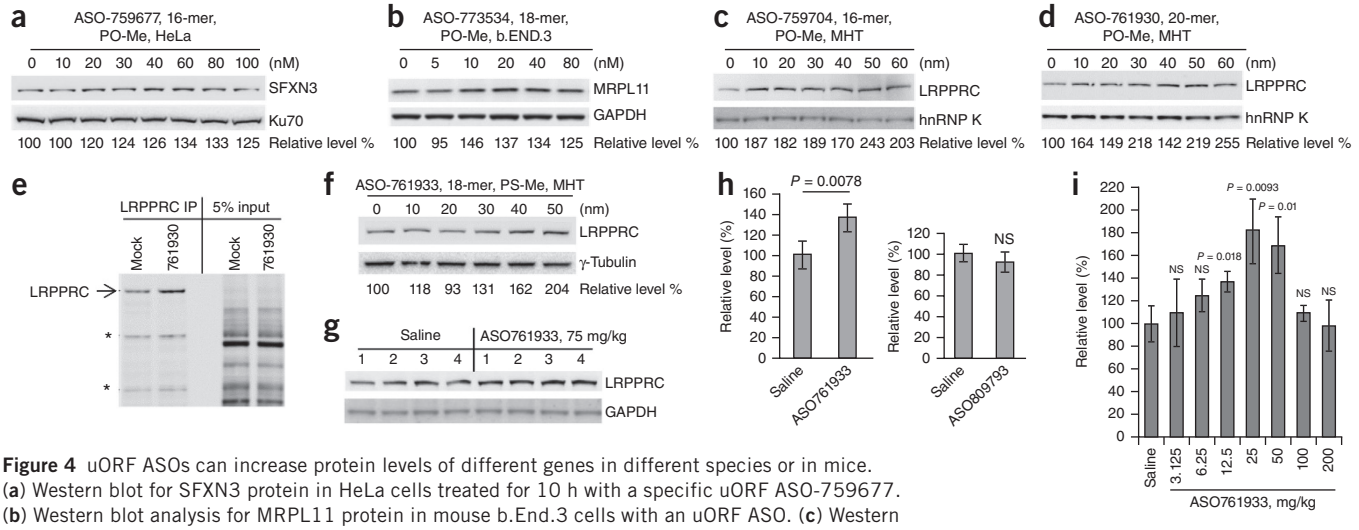

Figure 4 uORF ASOs can increase protein levels of different genes in different species or in mice. (**a**) Western blot for SFXN3 protein in HeLa cells treated for 10 h with a specific uORF ASO-759677. (**b**) Western blot analysis for MRPL11 protein in mouse b.End.3 cells with an uORF ASO. (**c**) Western blot for LRPPRC protein in mouse MHT cells treated for 10 h with a 16-mer uORF ASO. (**d**) Western analysis for LRPPRC protein levels in mouse MHT cells treated for 10 h with a 20-mer uORF ASO. (**e**) SDS-PAGE of LRPPRC protein immunoprecipitated from MHT cells treated or not treated with uORF ASO and were pulse-chase-labeled. Nascent proteins were detected by autoradiography. *, nonspecific proteins. (**f**) Western blot for LRPPRC protein in MHT cells treated with a PS-Me uORF ASO for 10 h. (**g**) Western blot for LRPRPC protein in liver homogenates of mice ($n = 4$) treated with uORF ASO-761933 for 48 h. (**h**) Quantification of relative LRPPRC protein levels from **g** (left) or **Supplementary Figure 9d** (right) compared to saline-treated mice. Error bars represent s.d. ($n = 4$ for left panel, $n = 3$ for right panel). (**i**) Relative LRPPRC protein levels in mice treated twice with indicated concentrations of the uORF ASO, based on the western blot results in **Supplementary Figure 9e**. Error bars represent s.d. ($n = 3$). *P* values were calculated based on unpaired *t*-test. NS, not significant. Lower protein bands in blots served as loading controls. Relative targeted protein ratios are listed below the blots. *In vitro* experiments were repeated at least twice, whereas the *in vivo* study was performed three times. Full-length blots are presented in **Supplementary Figure 13**.

beneficial[2,3,29]. Finally we note that uORF ASO position, chemistry and optimal dose must be experimentally determined for different targets or in different cell systems.

METHODS

Methods and any associated references are available in the online version of the paper.

Accession codes. Gene Expression Omnibus (GEO): GSE76343 (microarray analysis data).

Note: Any Supplementary Information and Source Data files are available in the online version of the paper.

ACKNOWLEDGMENTS

This work was supported by Ionis Pharmaceuticals internal funding. We thank M. Ramesh for technique assistance; H. Murray and C.L. De Hoyos for help in the animal study; S. Damle for microarray data processing and deposition; T. Reigle for help in figure preparation; and F. Bennett, E. Swayze, W. Lima and S. Wang for discussions.

AUTHOR CONTRIBUTIONS

X.L., W.S. and S.T.C. designed the research; X.L., W.S., H.S. and T.A.V. performed the experiments; and all authors analyzed the data. M.T.M. provided ASOs and measured T_m. X.L. and S.T.C. wrote the manuscript.

COMPETING FINANCIAL INTERESTS

The authors declare competing financial interests: details are available in the online version of the paper.

1. Crooke, S.T., Vickers, T., Lima, W. & Wu, H.-J. Mechanisms of antisense drug action, an introduction. In *Antisense Drug Technology - Principles, Strategies, and Application* (ed. Crooke, S.T.) 3–46 (CRC Press, 2008).
2. Hua, Y., Vickers, T.A., Baker, B.F., Bennett, C.F. & Krainer, A.R. Enhancement of SMN2 exon 7 inclusion by antisense oligonucleotides targeting the exon. *PLoS Biol.* **5**, e73 (2007).
3. Mourich, D.V. *et al.* Alternative splice forms of CTLA-4 induced by antisense mediated splice-switching influences autoimmune diabetes susceptibility in NOD mice. *Nucleic Acid Ther.* **24**, 114–126 (2014).
4. Pearson, S., Jia, H. & Kandachi, K. China approves first gene therapy. *Nat. Biotechnol.* **22**, 3–4 (2004).
5. Hoyng, S.A. *et al.* Gene therapy and peripheral nerve repair: a perspective. *Front. Mol. Neurosci.* **8**, 32 (2015).
6. Leader, B., Baca, Q.J. & Golan, D.E. Protein therapeutics: a summary and pharmacological classification. *Nat. Rev. Drug Discov.* **7**, 21–39 (2008).
7. Meng, L. *et al.* Towards a therapy for Angelman syndrome by targeting a long non-coding RNA. *Nature* **518**, 409–412 (2015).
8. Kozak, M. Pushing the limits of the scanning mechanism for initiation of translation. *Gene* **299**, 1–34 (2002).
9. Kozak, M. Evaluation of the "scanning model" for initiation of protein synthesis in eucaryotes. *Cell* **22**, 7–8 (1980).
10. Sonenberg, N. & Hinnebusch, A.G. Regulation of translation initiation in eukaryotes: mechanisms and biological targets. *Cell* **136**, 731–745 (2009).
11. Kozak, M. Regulation of translation via mRNA structure in prokaryotes and eukaryotes. *Gene* **361**, 13–37 (2005).
12. Araujo, P.R. *et al.* Before it gets started: regulating translation at the 5′ UTR. *Comp. Funct. Genomics* **2012**, 475731 (2012).
13. Pichon, X. *et al.* RNA binding protein/RNA element interactions and the control of translation. *Curr. Protein Pept. Sci.* **13**, 294–304 (2012).
14. Xue, S. & Barna, M. Specialized ribosomes: a new frontier in gene regulation and organismal biology. *Nat. Rev. Mol. Cell Biol.* **13**, 355–369 (2012).
15. Wethmar, K., Smink, J.J. & Leutz, A. Upstream open reading frames: molecular switches in (patho)physiology. *BioEssays: News and Reviews Mol. Cell. Dev. Biol.* **32**, 885–893 (2010).
16. Barbosa, C., Peixeiro, I. & Romão, L. Gene expression regulation by upstream open reading frames and human disease. *PLoS Genet.* **9**, e1003529 (2013).
17. Calvo, S.E., Pagliarini, D.J. & Mootha, V.K. Upstream open reading frames cause widespread reduction of protein expression and are polymorphic among humans. *Proc. Natl. Acad. Sci. USA* **106**, 7507–7512 (2009).
18. Lee, S. *et al.* Global mapping of translation initiation sites in mammalian cells at single-nucleotide resolution. *Proc. Natl. Acad. Sci. USA* **109**, E2424–E2432 (2012).
19. Suzuki, Y. *et al.* An upstream open reading frame and the context of the two AUG codons affect the abundance of mitochondrial and nuclear RNase H1. *Mol. Cell. Biol.* **30**, 5123–5134 (2010).
20. Liang, X.H., Sun, H., Shen, W. & Crooke, S.T. Identification and characterization of intracellular proteins that bind oligonucleotides with phosphorothioate linkages. *Nucleic Acids Res.* **43**, 2927–2945 (2015).
21. Deng, Y. *et al.* Therapeutic potentials of gene silencing by RNA interference: principles, challenges, and new strategies. *Gene* **538**, 217–227 (2014).

22. Freier, S.M. & Altmann, K.H. The ups and downs of nucleic acid duplex stability: structure-stability studies on chemically-modified DNA:RNA duplexes. *Nucleic Acids Res.* **25**, 4429–4443 (1997).
23. Seth, P.P. *et al.* Synthesis and biophysical evaluation of 2′,4′-constrained 2′O-methoxyethyl and 2′,4′-constrained 2′O-ethyl nucleic acid analogues. *J. Org. Chem.* **75**, 1569–1581 (2010).
24. Ling, J., Morley, S.J. & Traugh, J.A. Inhibition of cap-dependent translation via phosphorylation of eIF4G by protein kinase Pak2. *EMBO J.* **24**, 4094–4105 (2005).
25. Chiang, M.Y. *et al.* Antisense oligonucleotides inhibit intercellular adhesion molecule 1 expression by two distinct mechanisms. *J. Biol. Chem.* **266**, 18162–18171 (1991).
26. Pisareva, V.P., Pisarev, A.V., Komar, A.A., Hellen, C.U. & Pestova, T.V. Translation initiation on mammalian mRNAs with structured 5′UTRs requires DExH-box protein DHX29. *Cell* **135**, 1237–1250 (2008).
27. Koller, E. *et al.* Mechanisms of single-stranded phosphorothioate modified antisense oligonucleotide accumulation in hepatocytes. *Nucleic Acids Res.* **39**, 4795–4807 (2011).
28. Wethmar, K. The regulatory potential of upstream open reading frames in eukaryotic gene expression. *Wiley Interdiscip. Rev. RNA* **5**, 765–768 (2014).
29. Postina, R. *et al.* A disintegrin-metalloproteinase prevents amyloid plaque formation and hippocampal defects in an Alzheimer disease mouse model. *J. Clin. Invest.* **113**, 1456–1464 (2004).

ONLINE METHODS

Cell culture and transfection. HeLa, HEK293 cells (from Life Technologies), b.END.3 cells (from ATCC), and MHT cells without mycoplasma contamination were cultured in DMEM medium supplemented with 10% FBS at 37 °C incubator with 5% or 8% CO_2. One day before transfection, cells were seeded at ~40% confluency and incubated overnight. Transfection of ASOs was performed using Oligofectamine 2000 or RNAiMax (Life Technologies) for 10 h, unless otherwise indicated. Cells were then collected for protein or RNA analyses. For RNase H1 cleavage activity assay, cells transfected with uORF ASO-761909 for 10 h were reseeded at ~50% confluency, allowed to grow for 14 h, and then transfected again with ASO-462026 or ASO-110074. RNA was collected after 4 h. Transfection of luciferase or *DHX29* siRNAs (3 nM final concentration) was performed using RNAiMax (Life Technologies), based on manufacturer's instructions. At 24 h after siRNA transfection, cells were washed, and transfected with ASO-761909 for an additional 10 h. For the complementary oligonucleotide attenuation study, HeLa cells were transfected with ASO-761909 for 5 h, followed by transfection of oligonucleotide ASO-761929 for an additional 5 h. For cap-dependent translation inhibition, HeLa cells were transfected or not transfected with 25 nM ASO-761909 for 3 h, followed by addition of 10 μM 4E1Rcat (Sigma) for 7 h.

Western blotting. Mock-treated or cells treated with ASO were collected using trypsin and washed with PBS. The cell pellet was treated with RIPA buffer (Life Technologies), and cell lysate was prepared by centrifugation at 10,000*g* for 10 min at 4 °C. Proteins (20–40 μg/lane) were separated by 4–12% SDS-PAGE and transferred to membrane, and specific proteins were detected with primary and secondary antibodies and visualized using ECL. Protein quantification was performed using ImageJ, normalized to loading control protein, and the estimated ratios in percent are shown below the lanes in corresponding figures.

Polysome profile analysis. HeLa cells (5×10^6) were transfected with 25 nM ASO-761909 or control ASO-759704 for 7 h, followed by treatment with 100 μg/ml cycloheximide at 37 °C for 15 min. Cells were then washed three times with ice-cold PBS buffer containing 100 μg/ml cycloheximide and harvested, and cell pellet was resuspended in 800 μl lysis buffer (20 mM Tris pH 7.5, 5 mM $MgCl_2$, 100 mM KCl, 100 μg/ml cycloheximide, 2 mM DTT, 100 units of RNase inhibitor). Cells were incubated on ice for 5 min, vortexed, and 50 μl of 10% Triton X-100 and 50 μl of 10% sodium deoxycholate were added. Cells were incubated on ice for 5 min and cell extracts were cleared by centrifugation for 5 min at 12,000 r.p.m. 250 μl cell extract was loaded onto an 11 ml prechilled 7–47% continuous sucrose gradient. After centrifugation at 35,000 r.p.m. for 2 h at 4 °C using a SW41 rotor, fractions were taken at 400 μl each. RNA was prepared from 200 μl of each fraction using RNeasy (Qiagen), and used for qRT-PCR analysis for 28S rRNA, *RNASEH1* mRNA or *PTEN* mRNA (**Supplementary Fig. 5**). Alternatively, RNA was prepared from pooled fractions representing mono-ribosomes (fractions 9–12) and polysomes (fractions 15–25), and used for qRT-PCR (**Fig. 3c**).

RNA preparation and qRT-PCR. Total RNA was prepared from cells using RNeasy (Qiagen), based on manufacturer's protocol. qRT-PCR was performed in triplicate using TaqMan primer probe sets, and normalized to total RNA measured using SYBR Green (Life Technologies).

Protein stability assay. Mock-transfected HeLa cells or cells transfected with ASO-761909 for 12 h were treated with DMSO or 15 μg/ml cycloheximide for different times at 37 °C. Cells were then collected and cell lysates were prepared. Equal amounts of proteins were subjected to western blot analysis. A duplicate SDS-PAGE gel was silver-stained and served as loading control.

***In vivo* structural probing.** HeLa cells treated with ASO-761909 or ASO-783675 were incubated with 20 μl/ml dimethyl sulfate (DMS) at 37 °C for 3 min, followed by washing with cold 30% β-mercaptoethanol. The cell pellets were further washed with ice-cold PBS, and total RNA was prepared using RNeasy (Qiagen), based on the manufacturer's protocols. Primer extension was performed with 5 μg total RNA using a 5′ end-labeled primer XL403, as described previously[30]. The extension products were analyzed on an 8% polyacrylamide, 7 M urea gel. DNA sequencing reactions were performed using the same primer and a template plasmid containing the 5′ UTR sequence of *RNASEH1*.

Pulse-chase labeling and immunoprecipitation. Pulse-chase labeling was performed as described previously[31]. Briefly, HeLa cells grown in 15-cm dishes were transfected with different concentrations of ASO-761909 for 10 h, and incubated with prewarmed medium lacking methionine (Invitrogen, RPMI 1640) at 37 °C for 30 min. Cells were then pulse-labeled with 35 μCi/ml [S^{35}]methionine in RPMI1640 medium for 20 min and chased with 1 mM methionine for 40 min. Cells were washed with cold PBS containing 10 μg/ml cycloheximide and collected using trypsine. Cell lysates were prepared and equal amount of total protein was analyzed by SDS-PAGE, transferred to membrane, and visualized by autoradiography. For LRPPRC nascent protein detection, mouse MHT cells (1.5×10^7) were mock-transfected or transfected with ASO-751930 for 7 h, and pulse-chase labeled with [S^{35}]methionine as described above. Cells were then washed and cell lysate was prepared using IP buffer (Life Technologies), and immunoprecipitation was conducted using anti-LRPPRC antibody (Proteintech) at 4 °C for 3 h. After four washes, the precipitated proteins were analyzed on a 4–12% SDS-PAGE gel, transferred to a membrane, and visualized by autoradiography.

T_m analysis. The thermal stabilities of the duplexes formed by the oligonucleotides and a complementary RNA were analyzed by measuring the UV absorbance versus temperature curves as described previously[32]. Each sample contained 100 mM NaCl, 10 mM sodium phosphate (pH = 7.0), 0.1 mM EDTA, 4 μM oligonucleotide, and 4 μM complementary RNA (5′-CGCUGGGCCG GGAGUCGAAAUGCU).

***In vivo* study.** Seven-week-old male BALB/c mice ($n = 4$) without randomization were given a single dose of 75mg/kg ASO-761933 by subcutaneous injection. Animals were killed 48h later, and liver homogenates were prepared and subjected to western analysis by different investigators, in a blinded fashion. ASO-809793 was used as a control. In the dose-response study, ASO-761933 was administrated into mice ($n = 3$) at indicated doses, followed by another dose at the same level after 48 h. The animals were killed 48 h after the last dose. All tested animals were included in the analyses.

Construction of dual-luciferase reporters. PsiCheck-2 plasmid (Promega) was used as backbone for the reporter assay, with *Renilla* luciferase as reporter gene and firefly luciferase for normalization. For human RNase H1 reporter, the *RNASEH1* promoter and 5′ UTR region was amplified by PCR from genomic DNA using primers XL622 (5′-ACCGCTAGCTCACAGAGGAAC ACAACTTACCAC) and XL594 (5′-ACCGCTAGCCTCACTCCCGGCACC GGGA), and the PCR product was ligated to NheI site in PsiCheck-2, generating wild type RNase H1 reporter (PXL52). For ASO binding site mutation, PCR was performed using primers XL622 and XL601 (5′-ACCGCTAGCCT CACTCCCGGCACCGGGAAGCATAACCTCAGGCGGCCC AGCGTGGG CGCGAGCCGCCG), and ligated to NheI site of PsiCHECK-2 plasmid, generating plasmid PXL46.The underlined nucleotides are mutated sequences. For uAUG→uUUG mutation, PCR was performed using primers XL622 and XL606 (5′-ACCGCTAGCCTCACTCCCGGCACCGGGAAGCAATTCGAC TCCCGGCCCAGCGTGGGCGCGAGCCGCCG) that contains the single nucleotide mutation, and the PCR product was ligated to NheI site of psiCheck-2, generating plasmid PXL47. Human *RNASEH1* 3′ UTR region was amplified by PCR from genomic DNA using primers XL657 (5′-AAAGCGG CCGCCATGTGACTTTAGTCCTTGGG) and XL658 (5′-AAAGCGGCCGC AGAAGTGAGCCACTGTGCCCA), and the PCR product was ligated into Not I site of PXL46, PXL47 and PXL52, generating plasmids PXL55, PXL49 and PXL59,respectively. For stepwise mutation constructs, PCR reactions were performed using sense primer XL622, and antisense primers XL686 (5′-ACCGCTAGCCTCACTCCCGGCACCGGGAAGCATTTCGACTCCC GGGCCAGCGTGG GCGCGAGCCGCCG), XL687 (5′-ACCGCTAGCCTC ACTCCCGGCACCGGGAAGCATTTCGACTCCCGCGCCAGCGTGGGCG CGAGCCGCCG), XL688 (5′-ACCGCTAGCCTCACTCCCGGCACCGGGAA GCATTTCGACTCCCCCGCCAGCGTGGGCGCGAGCCGCCG), or XL689 (5′-ACCGCTAGCCTCACTCCCGGCACCGGGAAGCATTTCGACTCCGC CGCCAGCGTGGGCGCGAGCC GCCG), with plasmid PXL59 as a template.

The PCR products were digested with NheI, and ligated to the vector prepared by release of the wild-type insert from the NheI site of plasmid PXL59, generating plasmids PXL63 (M1), PXL64 (M2), PXL65 (M3) and PXL66 (M4), respectively. All plasmids were confirmed by sequencing.

For mouse *Mrpl11* reporter, the promoter and 5′ UTR region of *Mrpl11* was amplified using primers XL661 (5′-ACCGCTAGCCTTCGAAGT AGTCTCAGTCTGG) and XL636 (5′-ACCGCTAGCTAATCTTAGCT CGCCTCGGAGAAG), and the PCR product was ligated into NheI site of PsiCHECK-2, generating plasmid PXL53.

Reporter luciferase assay. HEK293 cells in 6-cm dishes were transfected with 0.2 μg plasmid (PXL59 or PXL49) for 24 h using Lipofectamine 3000 (Life Technologies), based on manufacture's instruction. Cells were then harvested and luciferase activity was measured using Dual-Glo Luciferase Assay system (Promega). Renilla luciferase activity was detected and normalized to firefly luciferase activity measured in the same samples. For uORF ASO effects on the luciferase reporter, HEK293 cells in 10-cm dishes were transfected for 24 h with 0.3–0.6 μg plasmids (PXL49, PXL59, PXL55, PXL63, PXL64, PXL65 or PXL66), using Lipofectamine 3000. Cells were split into 6-well plates and incubated for 8 h. ASOs were transfected at 30 nM (or as indicated in figure legends) using Lipofectamine RNAiMax (life Technologies). 16 h later, cells were harvested and luciferase activity was detected. The levels of the normalized reporter luciferase activity were calculated relative to the levels in mock transfected cells expressing the same reporter.

Subcellular fractionation. HEK293 cells in 15-cm dishes were transfected for 16 h with 25 nM ASO-761909 or control ASO-759704, using Lipofectamine RNAiMax. Cells were harvested and cytoplasmic/nuclear fractions were separated using PARIS kit (ThermoFisher), based on manufacturer's instructions. Cytoplasmic and nuclear RNA was prepared using RNeasy. Cytoplasmic mRNAs (*RNASEH1* and *DROSHA*) or nuclear RNA (*MALAT1*) were detected using qRT-PCR.

Reverse-transcription–PCR to detect RNase H1 splicing patterns. HeLa cells that were mock-transfected, or transfected with 25 nM ASO-761909 or control ASO-759704 for 16 h were harvested, and total RNA was prepared using RNeasy. RT-PCR was performed as described previously[33]. Briefly, reverse transcription was conducted using antisense primers specific to *RNASEH1* (XL560) or *PTEN* mRNA (reverse primer for primer-probe sets listed above). As a control, one set of reaction was performed without reverse transcriptase. With the cDNA as template, PCR was performed for 25 cycles using primers XL295 and XL296 (for exons 1–2) or XL295 and XL560 (for exons 1–3) for *RNASEH1* mRNA, or the primers for *PTEN* mRNA (listed above).

Detection of potential change in poly(A) length of *RNASEH1* mRNA. HeLa cells treated with different ASOs for 16 h were harvested, and total RNA was prepared using RNeasy. 5 μg total RNA were annealed with XL565 or XL563, and digested using *Escherichia coli* RNase H (NEB), as described previously[34]. After RNase H digestion, RNA was separated in an 8% PAGE and transferred to a membrane. The 3′ fragment of *RNASEH1* mRNA was detected by northern blot hybridization using a 5′-labeled probe XL564.

Microarray analyses. HeLa cells grown in 10-cm dishes were either mock-transfected, or transfected with 30 nM ASO-761909 or 30 nM control ASO-761932 for 15 h. Cells were harvested, and total RNA was prepared using RNeasy column (Qiagen), based on manufacturer's instructions. The total RNA was sent for microarray analyses performed by Phalanx Biotech. The significantly altered gene expression was defined with the absolute $\log_2$ ratio > 1 and $P < 0.05$. Genes showing significantly altered expression in ASO-761909 and ASO-761932 treated cells are listed in **Supplementary Tables 1** and **2**, respectively.

Antibodies. The following primary antibodies were purchased from Abcam: Ku70 (ab3114), hnRNP K (ab32969), ANXA2 (ab54771), SPPL2B (ab43856), FGFR1 (ab76464), eIF2a (ab26197), SFXN3 (ab181163), MRPL11 (ab127034) and LRPPRC (ab97505). The following antibodies were from Sigma: GAPDH (G8795) and γ-tubulin (T6557). A rabbit RNase H1 antibody was provided by H. Wu (from IONIS Pharmaceuticals). Anti-LRPPRC antibody (21175-1-AP, from Proteintech) was used for immunoprecipitation. DHX29 antibody (sc-81080) was from SCBT. These antibodies have been validated either previously (1DegreeBio) or by us using siRNA-mediated reduction and western blot analysis. Phosphorylated eIF2a (9721) were from Cell Signaling. Anti-rabbit (170-6515) and anti-mouse secondary (170-6516) antibodies were purchased from Bio-Rad.

30. Liang, X.H., Liu, Q. & Fournier, M.J. rRNA modifications in an intersubunit bridge of the ribosome strongly affect both ribosome biogenesis and activity. *Mol. Cell* **28**, 965–977 (2007).
31. Liang, X.H., Hart, C.E. & Crooke, S.T. Transfection of siRNAs can alter miRNA levels and trigger non-specific protein degradation in mammalian cells. *Biochim. Biophys. Acta* **1829**, 455–468 (2013).
32. Bleriot, Y. *et al.* Synthesis and acid catalyzed hydrolysis of B2,5 type conformationally constrained glucopyranosides: incorporation into a cellobiose analog. *Tetrahedron* **60**, 6813–6828 (2004).
33. Liang, X.H., Liu, Q. & Michaeli, S. Small nucleolar RNA interference induced by antisense or double-stranded RNA in trypanosomatids. *Proc. Natl. Acad. Sci. USA* **100**, 7521–7526 (2003).
34. Liang, X.H., Vickers, T.A., Guo, S. & Crooke, S.T. Efficient and specific knockdown of small non-coding RNAs in mammalian cells and in mice. *Nucleic Acids Res.* **39**, e13 (2011).

doi:10.1038/nbt.3589